



# Another transfer channel for shock energy flowing into intra-molecular: the coherent transfer channel

Cheng Tang<sup>1</sup> , Yunfei Song<sup>2</sup>, Zhaoyang Zheng<sup>2</sup>, Guoyang Yu<sup>2</sup>, Qiang Wu<sup>2</sup>, Yanqiang Yang<sup>1,2,3</sup>  and Zhe Lv<sup>1</sup>

<sup>1</sup> School of Physics, Harbin Institute of Technology, Harbin, 150001, People's Republic of China

<sup>2</sup> National Key Laboratory of Shock Wave and Detonation Physics, Institute of Fluid Physics, China Academy of Engineering Physics, Mianyang, 622900, People's Republic of China

E-mail: [yqyang@hit.edu.cn](mailto:yqyang@hit.edu.cn)

Received 28 June 2019, revised 13 November 2019

Accepted for publication 6 December 2019

Published 24 February 2020



## Abstract

In this paper, we have proposed that there is another transfer channel for shock energy flowing into intra-molecular vibration mode. During this energy transfer process, these higher frequency vibrations would gradually possess a coherence at the direction of shock wave. Namely, these optical phonons could be coherent after shock wave compressed. Based on the probe light can be scattered by the coherent optical phonons, a series of light scattering experiments at varying detection angles were performed to explore the existing evidence of coherent optical phonon in shocked materials. No matter the incident angle is  $6.2^\circ$  or  $15.7^\circ$ , the Signal intensity ratio  $\gamma_s$  and the line width  $\Gamma$  of compressed vibration were both showed peak value around the corresponding phase matching angle  $\theta'$ , which was attributed to the contribution of coherent optical phonons. Taken together, these experimental results demonstrated the existence of new proposed shock energy transfer channel, that coherent transfer channel, and open new perspectives in the molecular dissociation channel research in shocked materials.

Keywords: shock energy, Raman, phase matching

(Some figures may appear in colour only in the online journal)

## 1. Introduction

The energy transfer mechanism across multiple length and time scales is a fundamental challenge of energy science, and a transformational opportunity for high energetic materials researches [1]. Over past several decades, the energy transfer microscopic mechanism hidden behind shock front in crystal materials on molecular level has attracted increasing research attention, particularly in decomposition channel research [2–4]. The generally accepted microscopic theory believed that lower frequency lattice modes trend to be excited firstly by shock wave, namely, acoustic phonons are generated preferentially [5–8]. Then through the multi-phonon up pumping process, the shock energy flowing into higher

frequency vibrations [5–8]. It is worthy to note that the excited optical phonons in this process were thermal phonons [5–8]. When comparing with other energy transfer processes behind the shock wave, such as the local thermal equilibrium process and intra-molecular vibrational redistribution process, the multi-phonon up pumping process is a slower step and can be assumed as the limiting rate in the energy transfer process [6, 9, 10]. Inspired by the existence of coherent polarization wave in shocked materials [11–13], we proposed that there is another inter- to intra- molecular shock energy transfer channel, that it can be directly transfer into intra-molecular vibration modes. In this case, the higher frequency vibrations may be more appropriately described as optical phonons when considering its collective movement. Due to excited by the same shock wave, these optical phonons could gradually possess a coherence at the shock wave propagation direction

<sup>3</sup> Author to whom any correspondence should be addressed.

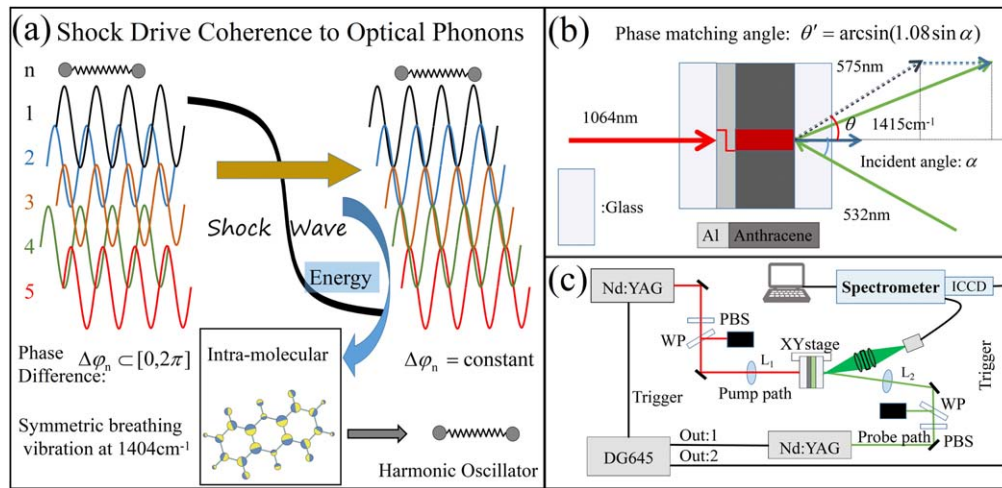


**Figure 1.** (a) The schematic diagram of shock drive coherence to optical phonons; (b) the phase matching diagram; (c) schematic diagram of the experimental setup.  $L_1$ ,  $L_2$ : Lens, PBS: polarizing beam splitter, WP: wave plate.

[6–8, 14]. Hence, the observation of coherent optical phonons in shocked materials could demonstrate the existence of the new proposed shock energy transfer channel.

The observation of phonons in real-time or non-real-time has been studied for many years [15, 16]. Note that the sample usually be sandwich structure for laser-driven shock wave [17, 18], the indistinct changes of transmission or reflection from other layers will be inputted into experimental results. Hence, these phonon observation methods shows poor performance in laser driven shock wave experiment. Inspired by some photon–phonon coupling experiments [19, 20], a series of light scattering experiments on nanosecond time scales were performed for the observation of coherent optical phonons.

## 2. Experimental section

As a typical aromatic molecule, there were lots of researches focus on the Hugoniot [21], fluorescence spectrum [22, 23], and other optical properties of anthracene molecule [24]. Due to the large Raman cross-section, narrow linewidth and high pressure-sensitive, the symmetric breathing vibration of anthracene molecule was widely used as a pressure probe in shocked materials [17, 18]. Meanwhile, note that the symmetric breathing vibration was belong to optical phonon, this vibration was also chosen as the research object in our observation experiment.

For stimulated Stokes Raman scattering experiment, a new physical quantity, which named intensity ratio  $\gamma$ , was defined as:  $\gamma(\theta) = I/I_0$ . Here,  $I$  is the intensity of one vibration at frequency  $\omega$  and  $I_0$  is the intensity of the symmetric breathing vibration at  $1404\text{ cm}^{-1}$  and  $\theta$  is the detection angle. Former stimulated Stokes Raman scattering experiment demonstrated the intensity ratio  $\gamma$  will be independent of detection angles  $\theta$ , which was also proved in our experiments [17, 18].

When a shock wave propagate through materials, it is reasonable to regard the shock wave as a one-dimensional

non-inertial force [25, 26]. Meanwhile, the intra-molecular vibrations, that the optical phonons, can be simplified as harmonic oscillators. The shock energy directly transfer into intra-molecular process, in essence, is the harmonic oscillators continually modulated by the shock induced force, as shown in figure 1(a). Due to modulated by the same shock induced force, these harmonic oscillators gradually possess a fixed phase difference. Namely, the optical phonons would gradually possess a coherence at the direction of force. Here, we prefer name this new proposed shock energy transfer channel as coherent transfer channel.

When the probe light arrived, the probe light could be scattered by these coherent optical phonons and then the corresponding scattering light generated at the phase matching angle, as shown in figure 1(b). According to the vector matching diagram, the relationship between incident angle  $\alpha$  and phase matching angle  $\theta$  can be described as:  $\theta' = \arcsin(1.08 \sin \alpha)$ . Due to the another pressure effect, that frequency red shift [17, 18], the coherent optical phonons only belong to the compressed part. Hence, the intensity ratio  $\gamma_s$  for the compressed symmetric breathing vibration at the phase matching angle  $\theta'$  can be expressed as:

$$\gamma_s(\theta') = \frac{I_R + I_P}{I_0} > \frac{I_R}{I_0} = \gamma_s(\theta). \quad (1)$$

Here, the  $I_R$  is the intensity of the compressed symmetric breathing vibration,  $I_P$  is the contribution of coherent optical phonons,  $\theta$  are other detection angles. It can be seen from the equation (1) that the intensity ratio  $\gamma_s$  of compressed symmetric breathing vibration at the phase matching angle  $\theta'$  is bigger than the values in other detection angles  $\theta$ . In addition, due to the lack of the interaction with shock wave, the uncompressed part was an excellent real-time background data in experiment, which was another important foundation of following experimental design and observation. Based on these theoretical analysis results, the core idea of our experiments is detecting the scattering light at different detection angles  $\theta$ , as shown in figure 1(c).

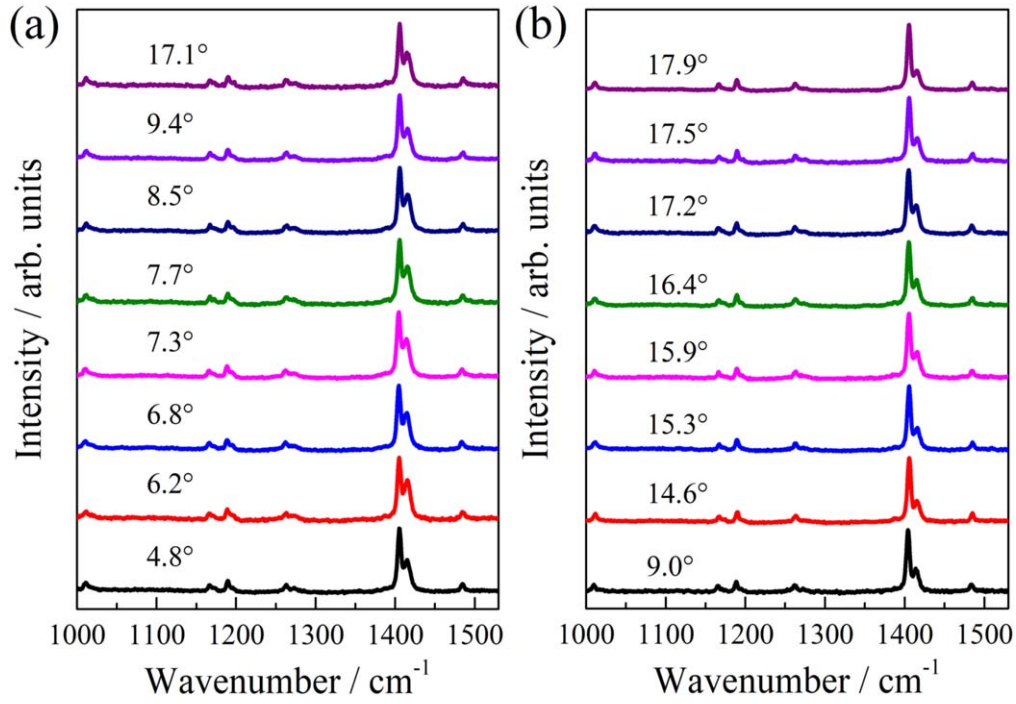


**Figure 2.** The detection angle dependence of the Raman spectrum of anthracene when the incident angle was (a) 6.2° and (b) 15.7°.

**Table 1.** The detailed information about observed vibrations.

Frequency(cm <sup>-1</sup> )	1009	1166	1189	1263	1404	1415	1485
Assignment	A <sub>1g</sub>	A <sub>1g</sub>	B <sub>1g</sub>	A <sub>1g</sub>	A <sub>1g</sub>	A <sub>1g</sub>	B <sub>1g</sub>
Type of vibration	C–H bending in plane	C–H bending in plane	C–H bending in plane	C–C stretching	Symmetric breathing	C–C stretching	C–C stretching

Before the observation of coherent optical phonons in shocked materials, the characterization of laser-driven shock wave propagation process was carried out firstly by time-resolved Raman spectroscopy. The shock wave loading and unloading processes in real-time was observed, but omitted here for the sake of brevity. The detailed information about this process, such as the preparing of sample, some important characteristics of laser and shock wave could be found in our former paper [17]. Based on our former research, the delay time between pump light and probe light was set as 35 ns in this research to better distinguish the compressed part from the uncompressed symmetric breathing vibration. The shock induced frequency red shift of symmetric breathing vibration was about 11 cm<sup>-1</sup> in this work, which the corresponding peak pressure was about 1.98 GPa.

### 3. Results and discussion

To explore the existence of coherent optical phonons, two different incident angles were selected as 6.2° and 15.7° respectively. When the incident angle  $\alpha$  is 6.2°, the scattering light around the phase matching angle 6.7° was observed. Similarly, when the incident angle changes to 15.7°, the scattering light was also observed around the corresponding

phase matching angle 16.8°. These spectral results were shown in figures 2(a) and (b) respectively.

The observed Raman spectrum contained seven different frequency vibrations, the C–H bending vibrations at 1009, 1166 and 1189 cm<sup>-1</sup>, the symmetric breathing vibration at 1404 cm<sup>-1</sup> and the C–C stretching vibration at 1263, 1415 and 1485 cm<sup>-1</sup> [27, 28]. In addition, the Raman spectrum of symmetric breathing vibration was split into double peak structure and the compressed part was red-shifted to 1415 cm<sup>-1</sup>. As a result, the C–C stretching vibration at 1415 cm<sup>-1</sup> was covered by the compressed symmetric breathing vibration, which can be observed at normal pressure [17, 27]. The detailed information about these vibrations are summarized in table 1 [27, 28].

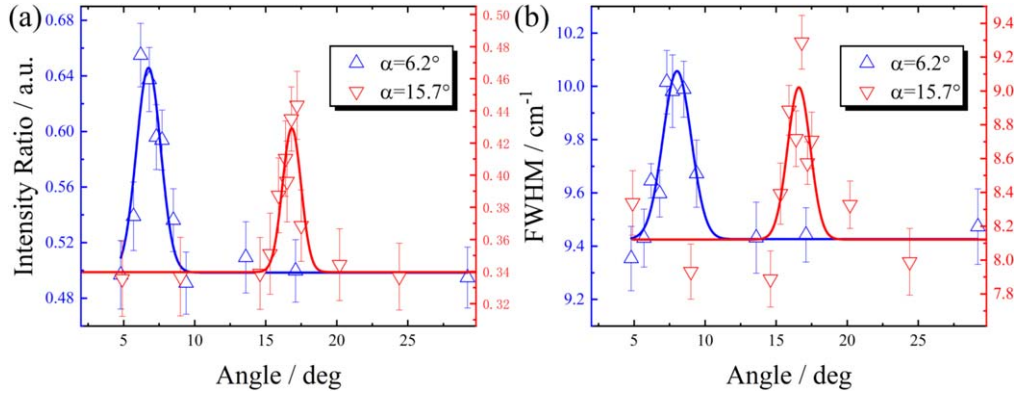
Despite the intensity of C–C stretching vibration at 1415 cm<sup>-1</sup> is negligible when compared with compressed symmetric breathing vibration, it is still necessary to explore its effect in our experiments. To this end, we rewrote the equation (1) as:

$$\gamma_s(\theta') = \frac{I_R + I_P + I_R^{C-C} + I_P^{C-C}}{I_0}. \quad (2)$$

Here,  $I_R^{C-C}$  is the intensity of C–C stretching vibration at 1415 cm<sup>-1</sup>,  $I_P^{C-C}$  is the contribution of corresponding coherent optical phonons. Here, we can regard the intensity

**Table 2.** The detailed information about detection angle dependence of intensity ratio.

Intensity ratio		Background				Signal
$\gamma_n = I_n/I_{1404\text{ cm}^{-1}}$		$\gamma_1 (1166\text{ cm}^{-1})$	$\gamma_2 (1189\text{ cm}^{-1})$	$\gamma_3 (1263\text{ cm}^{-1})$	$\gamma_4 (1485\text{ cm}^{-1})$	$\gamma_s (1415\text{ cm}^{-1})$
$\alpha = 6.2^\circ$	Max ( $\Delta\gamma$ )	0.02	0.02	0.02	0.01	0.15
	Mean ( $\gamma$ )	0.21	0.26	0.22	0.23	0.50
$\alpha = 15.7^\circ$	Max ( $\Delta\gamma$ )	0.01	0.01	0.01	0.01	0.10
	Mean ( $\gamma$ )	0.16	0.24	0.17	0.20	0.34

**Figure 3.** The detection angle dependence of the signal intensity ratio (a) and the FWHM (b) of compressed symmetric breathing vibration.

ratio at phase matching angle  $\theta'$  as two parts: the normal Stokes Raman scattering and the coherent phonons scattering. Let  $I'_R = I_R + I_R^{C-C}$  and  $I'_P = I_P + I_P^{C-C}$ , then we can still obtain this relationship:

$$\gamma_s(\theta') = \frac{I'_R + I'_P}{I_0} > \frac{I'_R}{I_0} = \gamma_s(\theta). \quad (3)$$

Thus, the intensity ratio  $\gamma_s$  at phase matching angle  $\theta'$  was confirmed to be larger than the values at other detection angles  $\theta$  again.

By Gaussian profile fitting, the detection angle dependence of intensity ratio  $\gamma$  were obtained respectively when the incident angles  $\alpha$  was  $6.2^\circ$  and  $15.7^\circ$ . For the sake of brevity, the vibrations whose frequency at 1166, 1189, 1263 and  $1485\text{ cm}^{-1}$  were all named as Background vibrations and the corresponding intensity ratios were also named as Background intensity ratios  $\gamma_n$  ( $n = 1, 2, 3, 4$ ). Furthermore, the compressed symmetric breathing vibration was named as Signal vibration and the corresponding intensity ratio was named as Signal intensity ratio  $\gamma_s$ . Whenever the incident angle  $\alpha$  is  $6.2^\circ$  or  $15.7^\circ$ , the Background intensity ratios  $\gamma_n$  all showed no correlation with detection angles  $\theta$  but only slightly fluctuated around the mean values. The detailed information about the detection angle dependence of Background intensity ratio was summarized in table 2 for better comparison. It can be seen from the table that the mean value of  $\gamma_2$  was slightly bigger than other Background intensity ratios. This discrepancy is mostly due to their different Raman cross-section. Moreover, the maximum deviation of these Background intensity ratios were about 0.02, which was less than the 10% of the mean value. These experimental data demonstrated that there was no peak structure in the detection angle dependence of Background intensity ratio in our

experiments. This result may be originated from two factors, the lower coherent phonon generation efficiency and the smaller scattering efficiency. Because of these two factors, the contribution of coherent optical phonon was limited and buried in background noise. In a word, these experimental data demonstrated the theoretical basis of coherent phonon observation experiment, that the intensity ratio will be a constant at varying detection angles  $\theta$  when there is no or little contribution of coherent phonons.

Next, we set out to explore the existence of a peak structure in the detection angle dependence of Signal intensity ratio  $\gamma_s$ . Since the symmetric breathing vibration of anthracene is very sensitive to pressure [17, 18], it is easy to determine the compressed symmetric breathing vibration from Raman spectrum. When the incident angle was  $6.2^\circ$ , the most obvious finding was that the Signal intensity ratio  $\gamma_s$  shown a peak value at detection angle  $6.7^\circ$ , which was the corresponding phase matching angle, as shown in figure 3(a) blue line. Moreover, the peak value of Signal intensity ratio  $\gamma_s$  has been reached up to 0.15, which was about six times higher than the maximum deviation  $\Delta\gamma_n$  of Background intensity ratios  $\gamma_n$ . This result suggested that the peak structure of Signal intensity ratio  $\gamma_s$  at the phase matching angle  $\theta'$  is a signal not noise. As such, when the incident angle  $\alpha$  changed to  $15.7^\circ$ , a peak structure of Signal intensity ratio  $\gamma_s$  was also observed at detection angle  $16.8^\circ$ , which was close to the corresponding phase matching angle  $17.0^\circ$ , as shown in figure 3(a) red line. Similarly, we measured the peak value of Signal intensity ratio  $\gamma_s$  and found it was about four times higher than the maximum deviation  $\Delta\gamma_n$  of Background intensity ratios  $\gamma_n$ . Taken together, at current time, we have the evidence to prove the existence of coherent optical phonons in shocked material. Considering the traditional multi-



**Table 3.** The detailed information about detection angle dependence of the linewidth of compressed symmetric breathing vibration at  $1415\text{ cm}^{-1}$ .

FWHM $\Gamma$ ( $\text{cm}^{-1}$ )	$\alpha = 6.2^\circ$		$\alpha = 15.7^\circ$	
	Max ( $\Delta\Gamma$ )	Mean ( $\Gamma$ )	Max ( $\Delta\Gamma$ )	Mean( $\Gamma$ )
$1415\text{ cm}^{-1}$	0.15	5.51	0.20	5.42

phonon up pumping process is a thermal process, the existence of coherent optical phonon indicated there is another transfer channel for shock energy flowing into intra-molecular.

As mentioned previously, the coherent optical phonon was demonstrated to have an important influence on the probe light scattering process. So we next explored the effect of coherent optical phonon in the detection angle dependence of linewidth. For stimulated Stokes Raman scattering experiment, many researches had demonstrated that the relationship between the linewidth and lifetime of Stokes peak can be expressed as:  $\Gamma/\hbar = 1/\tau$  [29–31], through the time-energy uncertainty relationship. Here, the  $\Gamma$  is the full width at half maximum (FWHM) of Stokes peak in units of  $\text{cm}^{-1}$ ,  $\hbar = 5.3 \times 10^{-12}\text{ cm}^{-1}\text{ s}$  and  $\tau$  is the lifetime of phonon. Research has demonstrated that the linewidth of Stokes Raman mode will be broadened by shock compression and show independent of detection angle [29–31]. To prove this we explored that the detection angle dependence of the linewidth of uncompressed symmetric breathing vibration in following experiment. When the coherent optical phonons taken into account, things changed a lot. Due to the coherent phonons have another relaxation channel [32, 33], that the coherence decay channel, its lifetime will be shorter than thermal phonons in same situation. Accordingly, the linewidth of coherent phonons will be bigger than thermal phonons. Based on these facts, there should be a peak value for Raman linewidth at the phase matching angle  $\theta'$  when the probe light was scattered by coherent optical phonons.

The linewidth of uncompressed symmetric breathing vibration at varying detection angles was shown in table 3. We have previously shown that the coherent optical phonons only belong to compressed vibration, thereby the uncompressed symmetric breathing vibration was still a perfect background data. It is obvious that no significant correlation between the linewidth of uncompressed symmetric breathing vibration and the detected angle was observed regardless of the incident angle is  $6.2^\circ$  or  $15.7^\circ$ . Furthermore, the corresponding maximum deviation of the FWHM of uncompressed vibration is about  $0.15\text{ cm}^{-1}$  and  $0.20\text{ cm}^{-1}$  respectively, when the incident angle is  $6.2^\circ$  and  $15.7^\circ$ . The smaller deviation around corresponding mean value indicated that there is no peak structure in the detection angle dependence of the linewidth of uncompressed symmetric breathing vibration. This interesting finding served as a proof-of-concept that the linewidth of Stokes Raman mode was

independent of detection angle when there is no coherent phonon.

Next, the analysis of the detection angle dependence of compressed symmetric breathing vibration was begun. Similarly, the effect of covered C–C stretching vibration at  $1415\text{ cm}^{-1}$  should be clarified firstly. As discussed above, the linewidth of Stokes Raman mode is independent of detection angle. Hence, all Raman modes which frequency at  $1415\text{ cm}^{-1}$ , that the compressed symmetric breathing vibration, the uncompressed and compressed C–C stretching vibration, will not produce a peak value in the detection angle dependence of linewidth when the contribution of coherent part was not taken into account. Namely, the observation of peak structure at phase matching angle could demonstrate the existence of coherent optical phonon. Here, we still name the Raman peak at  $1415\text{ cm}^{-1}$  as compressed symmetric breathing vibration for sake of discussion.

When the incident angle was  $6.2^\circ$  or  $15.7^\circ$ , the detected angle dependence of the linewidth of compressed symmetric breathing vibration was shown in figure 3(b). It can be seen from figure 3(b) that the FWHM of the compressed vibration showed a peak value around the phase matching angle  $6.7^\circ$  and the amplitude value reached up to  $0.6\text{ cm}^{-1}$ , which was two times higher than the maximum deviation of the linewidth of uncompressed vibration. In addition, a similar but not obvious peak structure has also appeared around the calculated phase matching angle  $16.8^\circ$ , when the incident angle change to  $15.7^\circ$ . Compared with the maximum deviation of the linewidth of uncompressed vibration, the peak value of the linewidth of compressed vibration was still larger. These data also suggest that the observed peak structure is a signal not noise. The two different performances of uncompressed and compressed vibration attest to a fact, that the linewidth would be broadened by the coherent optical phonons at the phase matching angle  $\theta'$ . This was another strong experimental evidence for the existence of coherent optical phonons in shocked materials.

The first observed peak structure of intensity ratio and linewidth both demonstrated the existence of coherent optical phonons in shocked materials, which cannot be generated by the traditional multi-phonon up pumping. Compared with the traditional channel, the new proposed shock energy transfer channel, that coherent transfer channel, have no need use the lattice modes as intermediation. Hence, the shock energy transfer rate in this channel is relatively fast, which can speed up the shocked induced chemical reaction. This property maybe used for the explanation of some materials show high chemical sensitivity when shock wave loading. The new proposed shock energy channel not only deepen the understanding of shock induced chemistry, but also shed some new light for the design of the next generation of energetic materials.

## 4. Conclusions

In this study, another shock energy transfer channel from inter- to intra- molecular in shocked materials was proposed.

Based on this viewpoint, the coherent optical phonons can be directly generated by shock wave, which was failed in the traditional multi-phonon up pumping process. Thus, the observation of coherent optical phonon could prove the existence of the new shock energy transfer channel. Considering the coherent optical phonon could be scattered by probe light, a series of light scattering experiment at various detection angle was designed to explore the existing evidence of coherent optical phonon. Interestingly, there was a remarkable peak value of intensity ratio at the corresponding phase matching angle regardless of the incident angle is  $6.2^\circ$  or  $15.7^\circ$ , which is the contribution of coherent optical phonons. When the attention focused on the linewidth of Raman mode, another strong evidence for the existence of coherent optical phonons was found. Experimental data show that the linewidth will be also broaden at the corresponding phase matching angle, which was another consequence for the probe light scattered by coherent phonon. Taken together, these results suggest that coherent optical phonon can be generated by shock wave. Namely, there is another transfer channel for shock energy flowing into intra-molecular. Compared with the traditional channel, the energy transfer rate for our new proposed channel is more larger and this discovery could open new perspectives in shock induced chemistry research.

## Acknowledgments

The National Natural Science Foundation of China (Grant Numbers 21673211 and 11372053) and the Science Challenging Program (Grant Number TZ2016001) support this work.

## ORCID iDs

Cheng Tang  <https://orcid.org/0000-0002-8906-7484>  
Yanqiang Yang  <https://orcid.org/0000-0003-4290-2793>

## References

- [1] Agrawal J P 1998 Recent trends in high-energy materials *Prog. Energy Combust.* **24** 1–30
- [2] Dang N C, Dreger Z A, Gupta Y M and Hooks D E 2010 Time-resolved spectroscopic measurements of shock-wave induced decomposition in cyclotrimethylene trinitramine crystals: anisotropic response *J. Phys. Chem. A* **114** 11560–6
- [3] Dreger Z A, Gruzdkov Y A, Gupta Y M and Dick J J 2014 Shock wave induced decomposition chemistry of pentaerythritol tetranitrate single crystals: time-resolved emission spectroscopy *J. Phys. Chem. B* **106** 247–56
- [4] Strachan A, Van Duin A C T, Chakraborty D, Dasgupta S and Goddard W A 2003 Shock waves in high-energy materials: the initial chemical events in nitramine RDX *Phys. Rev. Lett.* **91** 098301
- [5] Coffey C S and Toton E T 1982 A microscopic theory of compressive wave-induced reactions in solid explosives *J. Chem. Phys.* **76** 949–54
- [6] Zerilli F J and Toton E T 1984 Shock-induced molecular excitation in solids *Phys. Rev. B* **29** 5891
- [7] Dlott D D and Fayer M D 1990 Shocked molecular solids: vibrational up pumping, defect hot spot formation, and the onset of chemistry *J. Chem. Phys.* **92** 3798
- [8] Tokmakoff A, Fayer M D and Dlott D D 1993 Chemical reaction initiation and hot-spot formation in shocked energetic molecular materials *J. Phys. Chem.* **97** 1901
- [9] Hooper J 2010 Vibrational energy transfer in shocked molecular crystals *J. Chem. Phys.* **132** 014507
- [10] Fried L E and Ruggerio A J 1994 Energy transfer rates in primary, secondary, and insensitive explosives *J. Phys. Chem.* **98** 9786
- [11] Reed E J, Soljacić M, Gee R and Joannopoulos J D 2006 Coherent optical photons from shock waves in crystals *Phys. Rev. Lett.* **96** 013904
- [12] Reed E J, Armstrong M R, Kim K Y and Glowina J H 2008 Atomic-scale time and space resolution of terahertz frequency acoustic waves *Phys. Rev. Lett.* **101** 014302
- [13] Armstrong M R, Reed E J, Kim K Y, Glowina J H, Howard W M, Piner E L and Roberts J C 2009 Observation of terahertz radiation coherently generated by acoustic waves *Nat. Phys.* **5** 285
- [14] Eyring H 1978 Starvation kinetics *Science* **199** 740–3
- [15] Fu Z and Yamaguchi M 2016 Coherent excitation of optical phonons in GaAs by broadband terahertz pulses *Sci. Rep.* **6** 38264
- [16] Gambetta A *et al* 2006 Real-time observation of nonlinear coherent phonon dynamics in single-walled carbon nanotubes *Nat. Phys.* **2** 515
- [17] Tang C, Song Y, Liu X, Zhu X, Liu W, Yang Q, Lv Z and Yang Y 2018 Characterization of laser-driven shock compression by time-resolved Raman spectroscopy *Phys. Scr.* **94** 015401
- [18] Song Y, Zheng X, Yu G, Jun Z, Jiang L, Liu Y, Yang B and Yang Y 2011 The characteristics of laser-driven shock wave investigated by time-resolved Raman spectroscopy *J. Raman Spectrosc.* **42** 345–8
- [19] Alfano R R and Shapiro S L 1971 Optical phonon lifetime measured directly with picosecond pulses *Phys. Rev. Lett.* **26** 1247
- [20] Kang K, Ozel T, Cahill D G and Shim M 2008 Optical phonon lifetimes in single-walled carbon nanotubes by time-resolved Raman scattering *Nano Lett.* **8** 4642–7
- [21] Warnes R H 1970 Shock wave compression of three polynuclear aromatic compounds *J. Chem. Phys.* **53** 1088–94
- [22] Tang C, Zhu X, Song Y, Liu W, Yang Q, Lv Z and Yang Y 2019 Fluorescence temperature sensing based on thermally activated singlet-triplet intersystem crossing in crystalline anthracene *J. Appl. Phys.* **126** 054502
- [23] Tang C, Zhu X, Song Y, Liu W, Yang Q, Lv Z and Yang Y 2019 Revealing the origin of excimer emission in anthracene crystals: the role of excitation wavelength and pressure *J. Photochem. Photobiol. A* **376C** 263–8
- [24] Vaidya S N and Kennedy G C 1971 Compressibility of 18 molecular organic solids to 45 kbar *J. Chem. Phys.* **55** 987
- [25] Mathieu D, Martin P and La H J 2005 Simulation of the electron dynamics in shockwave and implications for the sensitivity of energetic materials *Phys. Scr.* **T118** 171
- [26] Mathieu D and Lucas A 2007 Computational approaches to the dynamics of ions and electrons in materials under extreme conditions *Comput. Mater. Sci.* **38** 514–21
- [27] Abasbegović N, Vukotić N and Colombo L 1964 Raman spectrum of anthracene *J. Chem. Phys.* **41** 2575–7
- [28] Beechem T and Graham S 2008 Temperature and doping dependence of phonon lifetimes and decay pathways in GaN *J. Appl. Phys.* **103** 093507

- [29] Zhao L, Baer B J and Chronister E J 1999 High-pressure Raman study of anthracene *J. Phys. Chem. A* **103** 1691–912
- [30] Bergman L, Alexson D, Murphy P L and Nemanich R J 1999 Raman analysis of phonon lifetimes in AlN and GaN of Wurtzite structure *Phys. Rev. B* **59** 12977
- [31] Kuball M, Hayes J M, Shi Y and Edgar J H 2000 Phonon lifetimes in bulk AlN and their temperature dependence *Appl. Phys. Lett.* **77** 1958–60
- [32] Vallée F 1994 Time-resolved investigation of coherent LO-phonon relaxation in III–V semiconductors *Phys. Rev. B* **49** 2460
- [33] Ganikhanov F and Vallée F 1997 Coherent TO phonon relaxation in GaAs and InP *Phys. Rev. B* **55** 15614